EJCB European Journal of Cell Biology **70**, 221–232 (1996, July) · © Wissenschaftliche Verlagsgesellschaft · Stuttgart

Adhesiveness of the apical surface of uterine epithelial cells: the role of junctional complex integrity

Michael Thie[1)a*], Petra Fuchs[a*], Stefan Butz[b], Frank Sieckmann[c], Heinz Hoschützky[d], Rolf Kemler[d], Hans-Werner Denker[a]

[a] Institute of Anatomy, University of Essen Medical School, Essen/Germany
[b] Howard Hughes Medical Institute, University of Texas, Dallas, TX/USA
[c] Institute of Radiation Biology, University of Essen Medical School, Essen/Germany
[d] Max Planck Institute for Immunobiology, Freiburg i.Br./Germany

Received November 16, 1995
Accepted January 29, 1996

Uterine epithelium – epithelial polarization – junctional complex – adhesiveness

Embryo implantation necessitates that the apical plasma membrane of uterine epithelial cells acquires adhesiveness. Recent studies have indicated that modulation of a major element of the epithelial phenotype, i.e. apical-basal cell polarity, might be critical in this respect. Here, we analyze polar characteristics of nonadhesive vs. adhesive uterine epithelial cell lines focusing on cytoskeletal-junctional interactions that may play a role in regulating adhesiveness of the apical plasma membrane.

HEC-1-A is a human uterine epithelial cell line exhibiting nonadhesive properties of its apical surface for trophoblast, whereas RL95-2 represent another such cell line exhibiting adhesive properties enabling trophoblast attachment. Homotypic intercellular contacts and functionally related proteins, i.e. ZO-1, E-cadherin, α-catenin, β-catenin, plakoglobin, and desmoplakin I, were examined by transmission electron microscopy, immunocytochemistry, confocal laser scanning microscopy, and immunoprecipitation techniques. In addition, details of actin filament architecture were studied after phalloidin labeling. While nonadhesive HEC-1-A exhibited the well-known pattern of cell-to-cell contacts of polarized epithelial cells, adhesive RL95-2 showed a lack of ZO-1 expression, tracer leakiness of the paracellular pathway, and atypical features in adherens junctions: E-cadherin, α-catenin and plakoglobin were colocalized in all plasma membrane domains and β-catenin was localized in lateral membrane domains. Immunoprecipitations showed in both cell lines the presence of two different E-cadherin-catenin complexes, one composed of E-cadherin, α-catenin and β-catenin, and the other of E-cadherin, α-catenin and plakoglobin. Concerning RL95-2 these data indicate that E-cadherin/plakoglobin complexes are randomly distributed, whereas E-cadherin/β-catenin complexes are laterally localized in these cells. Additionally, the actin-based cytoskeleton of RL95-2 lacked a polar organization. With respect to the intermediate filament-desmosome system, both cell types expressed desmoplakin I, but the vast majority of RL95-2 lacked well-formed desmosomes as demonstrated by electron microscopy.

It is concluded that modulation of tight junctions and/or remodelling of adherens junctions, e.g. differential distribution of E-cadherin/plakoglobin complexes and E-cadherin/β-catenin complexes, are correlated with the development of apical adhesiveness of human uterine epithelial cells. This model system should allow to test experimentally whether this correlation is due to any causal function in the development of epithelial cell polarity.

Introduction

Embryo implantation in mammals and in the human requires adhesiveness of the apical plasma membrane of uterine epithelial cells thus enabling the initial contact between the embryo and maternal tissues. Human uterine epithelial cells show a polarized phenotype as typical for all simple epithelia including organization of the surface membrane into biochemically distinct apical and basolateral plasma membrane domains. The basolateral membrane domain is studded with various adhesion molecules, including E-cadherin and integrins, mediating stable adhesion to neighboring cells or to the extracellular matrix. The apical domain is largely free of these molecules and nonadhesive for opposing uterine epithelial cells or embryonic cells such as trophoblast. Interestingly, the apical domain can be functionally reprogrammed towards adhesiveness for trophoblast when cells are exposed to an appropriate hormonal milieu (for reviews, see [10, 16, 38]).

The molecular details of how the surface of human uterine epithelial cells contacts trophoblast are still unclear. There is evidence that alterations in membrane compositions of uterine cells occur in a concerted way in both apical and basolateral domains and are coupled somehow with a partial loss of epithelial characteristics thus leading to acquisition of apical

---

[1)] Dr. Michael Thie, Institut für Anatomie, Universitätsklinikum, Hufelandstr. 55, D-45122 Essen/Germany.

[*] M. Thie and P. Fuchs contributed equally to this study.

adhesiveness of epithelial cells [10, 11]. For example, establishment of apical adhesiveness of human uterine cells in vivo is correlated with redistribution of α6-integrin subunits from the basal to the lateral subdomain and a significant increase of CD44 expression in the lateral domain [1]. A reduction in the thickness of the glycocalyx and in the cell surface charge of the apical membrane domain seems to be related to these alterations [26]. Cell culture studies have shown that apical adhesiveness for trophoblast of a human uterine-derived cell line, i.e. RL95-2 cells, correlates with the occurrence of α6-, β1- and β4-integrin subunits at the entire surface membrane, whereas polarized distribution of integrins correlates with nonadhesiveness of the apical membrane in HEC-1-A cells [51]. The common denominator of these changes might be a so far non-identified mechanism modulating the apical-basal cell polarity ultimately leading to adhesiveness of the apical plasma membrane of uterine epithelial cells for trophoblast [10–12]. The present study was designed in order to get insight into features involved in modulation of cell polarity in uterine cells.

Materials and methods

Materials

All chemicals were of analytical grade and were obtained from Merck, Darmstadt/Germany or Sigma-Aldrich, Deisenhofen/Germany.

Cell culture

Human endometrial carcinoma cells were purchased from the American Type Culture Collection (ATCC; Rockville, MD/USA), i.e. HEC-1-A cells (HTB 112) and RL95-2 cells (CRL 1671). Cell lines were grown in plastic flasks in 5% CO_2-95% air at 37 °C. HEC-1-A cells were seeded out in McCoy's 5A medium (Biochrom Seromed, Berlin/Germany) supplemented with 10% fetal calf serum (Gibco-Life Technologies, Eggenstein/Germany), and RL95-2 cells in a 1+1 mixture of Dulbecco's modified Eagle's medium (Gibco) and Ham's F12 (Biochrom) supplemented with 10% fetal calf serum. All media were additionally supplemented with penicillin (100 IU/ml; Boehringer, Mannheim/Germany) and streptomycin (100 µg/ml; Boehringer, Mannheim/Germany). The growth medium was changed every 2 to 4 days, and cells were subcultured by trypsinization (trypsin-EDTA solution; Gibco) when they became confluent.

For metabolic labeling experiments, monolayers (2×10^7 cells) were grown in methionine-free medium (Gibco), supplemented with 10% dialyzed fetal calf serum, for 2 h prior to the addition of 50 µCi/ml $[^{35}S]$methionine (Amersham, Braunschweig/Germany) for overnight incubation.

Adhesiveness of confluent monolayers for human JAR choriocarcinoma cell spheroids (ATCC: HTB 144) was routinely measured using a centrifugal force-based adhesion assay [27]. Confirming recently published data [51], RL95-2 monolayers allowed JAR cells to attach while HEC-1-A monolayers did not (not shown).

Antibodies

Junctional complexes. Rabbit polyclonal antibodies to human ZO-1 (61-7300) were obtained from WAK Chemie, Bad Homburg/Germany. Mouse monoclonal antibody to human E-cadherin (6F9; [14]) was donated by Dr. J. Behrens (Max-Delbrück-Centrum, Berlin/Germany). Preparation of rabbit polyclonal antibodies to uvomorulin (E-cadherin; [41]), to peptides of α-catenin (αM12K; [21]), β-catenin (βP14L; [5]), and plakoglobin (D15A; [4]) has been described previously. Mouse monoclonal antibody directed against desmoplakin (desmoplakin I; [7]) was a gift of Dr. J. Kartenbeck (DKFZ, Heidelberg/Germany).

Cytoskeleton. Mouse monoclonal antibodies to cytokeratin 7 (Ks 7.18), to cytokeratin 8 (Ks 8.7), to cytokeratin 18 (Ks 18.04), and to cytokeratin 19 (Ks 19.1) were obtained from Progen, Heidelberg/Germany, and a mouse monoclonal antibody to vimentin (V9) from Sigma-Aldrich, Deisenhofen/Germany.

Preparation of cytoskeletal material and immunoblotting

Intermediate filament-enriched fractions were obtained from confluent monolayers according to Eckert and Kartenbeck [13]. Monolayers (2×10^7 cells) were washed three times with phosphate buffered saline (PBS) at room temperature and subsequently immersed in 2 ml high salt buffer (10 mM Tris-HCl, pH 7.5, 1.5 M KCl, 140 mM NaCl, 5 mM EDTA, 1% Triton X-100, 1 mM phenylmethylsulfonyl fluoride, 1 mM dithioerythritol, 1.5 µM pepstatin A). Cell extracts were prepared by sonication of cells and stirring of suspension for 20 min at 4 °C followed by centrifugation at 5000*g* for 20 min at 4 °C. The pelleted cytoskeletal material was washed twice with PBS and used for sodium dodecyl sulfate (SDS) polyacrylamide gel electrophoresis (PAGE) under reducing conditions [28].

For immunodetection, proteins separated by SDS-PAGE were transferred electrophoretically to Immobilon membrane (Millipore, Bedford, MA/USA). Filters were immersed in 25 mM Tris-HCl, pH 7.4, 150 mM NaCl, 30 mM KCl, 0.1% Tween 20, at 37 °C for 1 h, incubated with 2 to 5 µg/ml primary antibody and then with alkaline phosphatase-conjugated secondary antibody (Dianova, Hamburg/Germany). Bound antibodies were detected using Nitro blue tetrazolium and 5-bromo-4-chloro-3-indolyl phosphate as substrates (Sigma-Aldrich).

Preparation of cell lysates and immunoprecipitation

Cell lysates were obtained from confluent monolayers according to Butz and Kemler [3]. Monolayers (2×10^7 cells) were washed three times with PBS at room temperature and subsequently immersed in 800 µl cold lysis buffer (20 mM imidazole, pH 6.8; 100 mM KCl, 2 mM $MgCl_2$, 10 mM ethylene glycol-bis(β-aminoethyl ether)N,N,N′,N′-tetraacetic acid, 300 mM sucrose, 1 mM Na-vanadate, 1 mM Na-molybdate, 1 mM Na-fluoride, 0.2% Triton X-100, 1 mM phenylmethylsulfonyl fluoride, 1 mM N-ethylmaleimide, and 1.5 µM pepstatin A) for 10 min at 4 °C. Cell lysates were centrifuged at 16000*g* for 10 min and supernatant was precleared by incubation for 1 h with 250 µl/ml supernatant of 10% (w/v) protein A-Sepharose beads (Pharmacia, Freiburg/Germany) preabsorbed with lysis buffer containing ovalbumin (1 mg/ml). Final lysates were centrifuged at 1000*g* for 5 min followed by centrifugation at 16000*g* for 5 min.

For immunoprecipitation, precleared supernatants of cell lysates equivalent to 4×10^6 cells were incubated with the appropriate antibody (5 µg anti-uvomorulin, 10 µg anti-α-catenin, 30 µg anti-β-catenin and 20 µg anti-plakoglobin) and 50 µl protein A-Sepharose for 1 h.

Fig. 1. Ultrastructure of HEC-1-A and RL95-2 monolayers cultivated on poly-D-lysine-coated coverslips. HEC-1-A cells (**a**) form close lateral membrane contacts and are highly polarized, e.g. the nucleus is located predominantly basally, organelles in the supranuclear region. Note numerous microvilli at the apical cell pole (*arrows*). RL95-2 cells (**b**) grow as monolayers of irregular shape and show little signs of polar organization, e.g. the nucleus is located in the center, organelles tend to pile up perinuclearly. Microvilli are largely lacking. – **c, d.** Photomicrographs of ultrathin sections of lateral plasma membranes of HEC-1-A cells (**c**) and RL95-2 cells (**d**). Note that HEC-1-A cells but not RL95-2 cells form morphologically distinct tight junctions, intermediate junctions and desmosomes. – oo Coverslip. – *Stars:* Growth medium. – N Nucleus. – tj Tight junction. – ij Intermediate junction. – d Desmosome. – H1, H2 HEC-1-A cells. – R1, R2 RL95-2 cells. – Bars 5 µm (**a, b**), 0.25 µm (**c, d**).

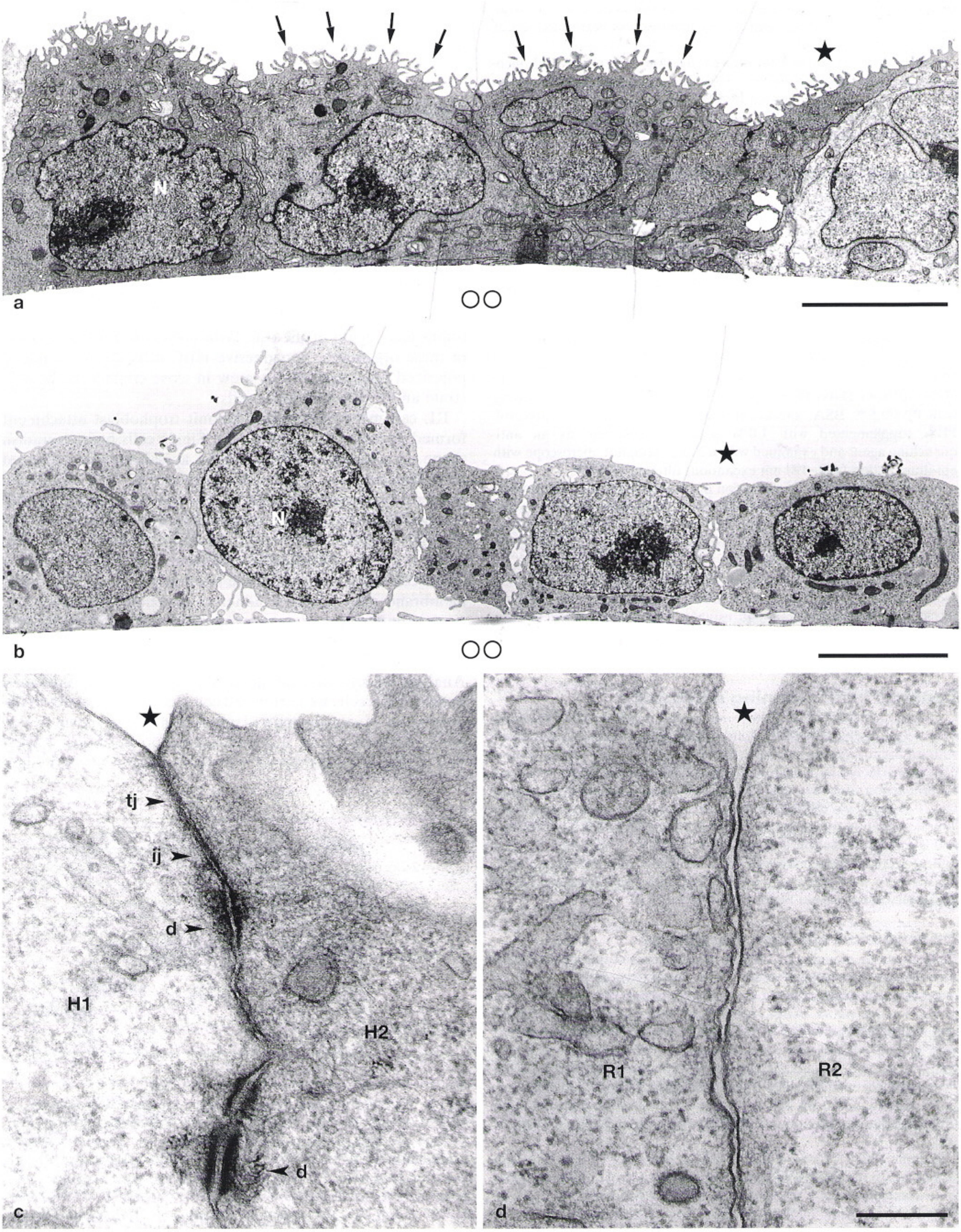
★
N
a
○○
★
N
b
○○
★
tj
ij
d
H1
H2
d
c
★
R1
R2
d

Beads were washed 5 times with lysis buffer supplemented with ovalbumin. SDS-PAGE of the immunoprecipitates was performed under reducing conditions [28].

For fluorography, SDS-PAGEs were fixed in 10 % acetic acid, incubated with 1 M Na-salicylate and subsequently dried. For immunodetection, the proteins separated by SDS-PAGE were transferred electrophoretically to Immobilon membrane. Transferred proteins were detected by appropriate primary antibodies as described above.

Immunofluorescence and phalloidin staining

Monolayers grown on poly-D-lysine-coated glass coverslips were rinsed twice in PBS, fixed and permeabilized by incubation in 96 % methanol-water for 7 min at − 20 °C. After several washings with PBS and a final wash in PBS/0.5 % bovine serum albumin (BSA), cells were incubated for 40 min at room temperature with the primary antibody. Thereafter, cells were rinsed in PBS/0.5 % BSA (3 × 5 min) and incubated with the corresponding fluorescein isothiocyanate (FITC)-conjugated secondary antibody for 40 min at room temperature. FITC-conjugated swine anti-rabbit secondary antibodies (F205), FITC-conjugated rabbit anti-mouse secondary antibodies (F232) and FITC-conjugated rabbit anti-rat secondary antibodies (F234) were obtained from Dako Diagnostika, Hamburg/Germany. After rinsing with PBS/0.5 % BSA, specimens were mounted with 90 % glycerol-PBS, supplemented with 1.0 % p-phenylenediamine as an anti-quenching agent and examined with a Zeiss Axiophot microscope with epi-illumination (450–490 nm excitation; filterset 487909).

For phalloidin staining, a solution of tetramethylrhodamine isothiocyanate (TRITC)-conjugated phalloidin (Sigma-Aldrich) at a concentration of 25 μg/ml in PBS was used. Monolayers grown on poly-D-lysine-coated glass coverslips were rinsed in PBS, fixed with 3 % paraformaldehyde for 15 min at room temperature, permeabilized by incubation for 2 min in a solution of 0.05 % Triton X-100, and then incubated for 15 min in a solution of TRITC-phalloidin. After rinsing, the stained cells were examined using a Zeiss Axiophot microscope equipped with epi-illumination (530-585 nm excitation; filterset 487900).

Confocal laser scanning microscopy

Confocal microscopy was carried out using a confocal laser scanning microscope (Leitz DM RBE; Leica, Heidelberg/Germany) equipped with an argon krypton ion laser. For experiments, 488 nm excitation light was selected by a narrow bandpass interference filter. A 40-fold oil immersion objective (PL FLUOTAR) with a numerical aperture from 0.5 to 1.0 was chosen. In the laser scanning mode the theoretical lateral resolution was calculated to be 0.2 μm (NA = 1.0; λ = 488 nm) and the axial resolution 0.22 μm (NA = 1.0; λ = 488 nm). Vertical optical sections were computed from x-z scans with 512 lines/image. Photographs were taken with an APX-100 film (Agfa Gevaert, Leverkusen/Germany) from a black and white monitor.

Transmission electron microscopy

Cells grown as monolayers on poly-D-lysine-coated thermanox coverslips (Nunc, Naperville, IL/USA) were rinsed twice in PBS and fixed in 2.5 % glutaraldehyde in 0.1 M cacodylate buffer, pH 7.4, for 30 min at room temperature. After repeated washings in cacodylate buffer, samples were fixed with 1 % OsO_4 in cacodylate buffer, dehydrated with graded ethanol and propylene oxide, and embedded in epoxy resin mixture [8]. The embedded monolayers were separated from the thermanox coverslips by snap freezing in liquid nitrogen. Ultrathin sections were mounted on 200-mesh copper grids, double stained with uranyl acetate and lead citrate, and examined with a Philips EM 400 at 80 kV.

In some cultures ruthenium red (4527.1; Roth, Karlsruhe/Germany) was added to the fixative applied to the apical side of confluent monolayers. Samples were washed twice in PBS and fixed in 2.5 % glutaraldehyde in cacodylate buffer, containing 0.1 % ruthenium red for 1 h at 4 °C. After several washings (3 × 3 min) in cacodylate buffer, samples were postfixed with 1 % OsO_4 in cacodylate buffer containing 0.1 % ruthenium red for 3 h at room temperature [31]. Then samples were dehydrated in ethanol and propylene oxide, embedded in epoxy resin mixture and examined as described above omitting double-staining with uranyl acetate and lead citrate.

Results

Polarized vs. nonpolarized epithelial phenotype

Ultrastructure. Low magnification overviews of ultrastructure of HEC-1-A and of RL95-2 cells are shown in Figure 1. HEC cells which are nonadhesive for trophoblast-type cells formed ordered monolayers of cuboidal to columnar cells (Fig. 1a). The apical surface was covered with numerous, relatively short microvilli. Nuclei of HEC cells were predominantly located at the base of the cell. Mitochondria, Golgi apparatus, and endoplasmic reticulum were mostly positioned in the supranuclear region of the cell. With respect to the distribution of these organelles, nonadhesive HEC cells showed a highly polarized phenotype. Cells grew in close contact to the substrate and to adjacent HEC cells.

RL cell monolayers which permit trophoblast attachment formed irregular sheets (Fig. 1b). Single cells had a roundish shape. In contrast to HEC cells, the apical cell pole appeared dome-like and was largely free of microvilli. The cell nuclei were predominantly located in the center of the cell, and organelles tended to pile up perinuclearly without showing any sign of polar distribution. RL cells adhered to the substrate via large cytoplasmic extensions but did not form a broad cell-matrix contact at the basal cell pole. At the lateral membrane only primitive adherens junctions were seen; regions of interacting plasma membranes were alternating with regions of large intercellular spaces. Thus, RL cells lacked the structural polarization as typical for a simple epithelium.

Analysis of cytoskeletal proteins. To prove the epithelial nature of RL cells we performed cell typing with respect to the expression of intermediate filament proteins as shown in Figure 2. SDS-PAGE of the cytoskeletal preparations showed four major polypeptides of molecular weight 54 000 Dalton

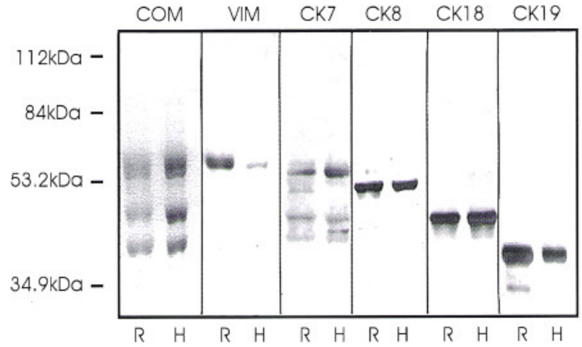

Fig. 2. SDS-PAGE and Western blots of cytoskeletal proteins of HEC-1-A cells (H) and RL95-2 cells (R). Coomassie Blue staining (COM) and immunoreactions with antibodies to vimentin (VIM), to cytokeratin 7 (CK7), 8 (CK8), 18 (CK18) and 19 (CK19). The proteins were resolved using 7.5 % acrylamide gels. Prestained reference proteins used for coelectrophoresis are phosphorylase B (112 000 Da), bovine serum albumin (84 000 Da), ovalbumin (53 200 Da), and carbonic anhydrase (34 900 Da). Note that the same pattern of cytokeratin polypeptides and vimentin is found in both HEC-1-A cells and RL95-2 cells.

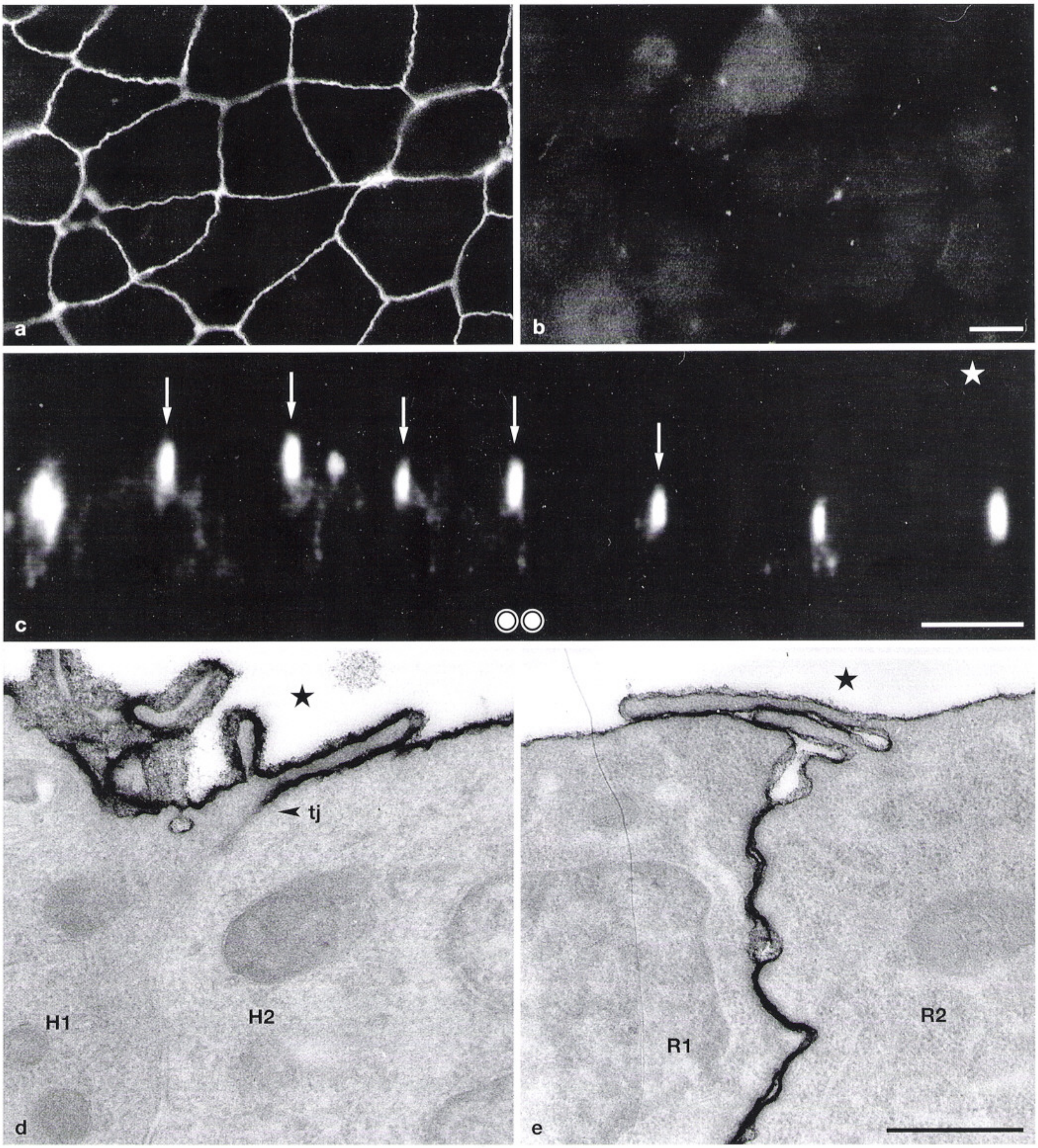

Fig. 3. Immunostaining of HEC-1-A monolayers (**a**, conventional microscopy; **c**, confocal vertical image) and RL95-2 monolayers (**b**, conventional microscopy) with antibodies to ZO-1; note that HEC-1-A cells but not RL95-2 cells are positive for ZO-1. *Arrows* mark the position of cell-to-cell contacts in monolayers (**c**). Photomicrographs of ultrathin sections of HEC-1-A cells (**d**) and RL95-2 cells (**e**) following ruthenium red labeling; ruthenium red penetrates into the lateral intercellular space in RL95-2 cells but not in HEC-1-A cells. – oo Coverslip. – *Stars:* Growth medium. – H1, H2 HEC-1-A cells. – R1, R2 RL95-2 cells. – Bars 10 μm (**a, b**), 10 μm (**c**), 0.5 μm (**d, e**).

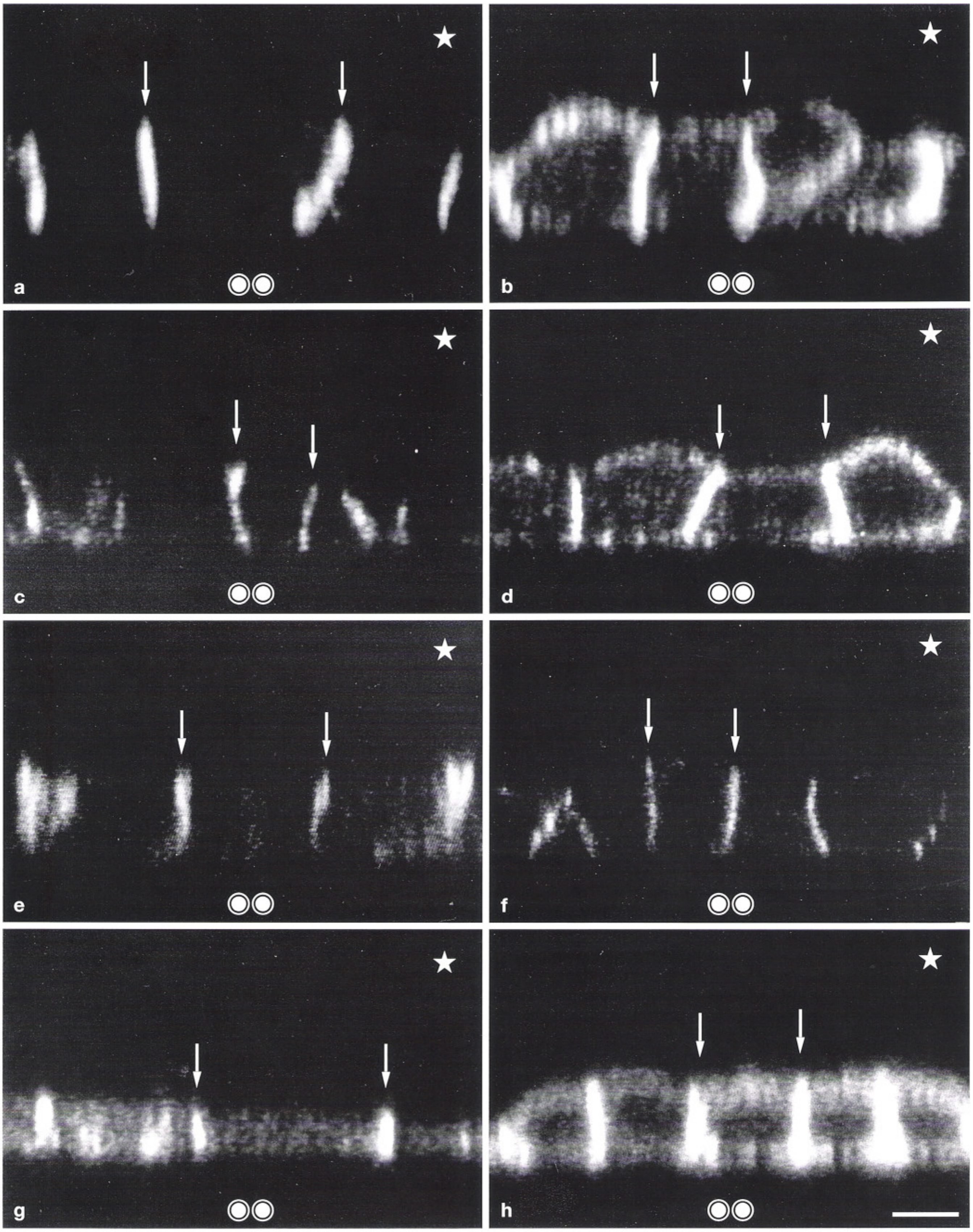
★
a
◎◎
★
b
◎◎
★
c
◎◎
★
d
◎◎
★
e
◎◎
★
f
◎◎
★
g
◎◎
★
h
◎◎

(Da), 52000 Da, 45000 Da, and 40000 Da. In Western blots with cytokeratin antibodies cytokeratins 7 (54000 Da), 8 (52000 Da), 18 (45000 Da), and 19 (40000 Da) were identified. Vimentin also gave a weak band (57000 Da) although not being detected by immunohistochemistry formerly [51]. The same pattern of cytokeratin polypeptides and in contrast to former studies (see above) also vimentin is found in cytoskeletal residues from polarized HEC cells (Fig. 2). Thus, a cytokeratin polypeptide pattern consisting of components 7, 8, 18, 19 as well as vimentin has been found for both, nonpolarized RL cells and polarized HEC cells, indicating their origin from single-layered endometrial epithelium known to contain these cytoskeletal proteins [35, 37].

Structure of epithelial junctional complexes

Tight junctions. The lateral plasma membranes of adjacent HEC cells are aligned in parallel and form in their subapical part characteristic tight junctional membrane contacts consisting of a series of fusion spots (Fig. 1c). In freeze fractures, the tight junction structures appeared as smooth strands on the protoplasmic face of the replica and as furrows on the exoplasmic face of the replica (data not shown). Using immunohistochemistry, the tight junction protein ZO-1 was likewise found at the subapical part of the lateral border of adjacent cells (Figs. 3a, c). Ruthenium red added to the apical side of HEC monolayers stained intensely the apical cell surface including the membrane of luminal vesicles and the content of many apparently cytoplasmic vesicles, but no staining was observed beyond the level of the junctional contact points (Fig. 3d) thus proving that these junctions were indeed an effective penetration barrier.

In contrast to HEC cells, no characteristic tight junctions were seen at the membrane contacts of adjacent RL cells in transmission electron microscopy (Fig. 1d). Also in freeze fractures tight junction strands were never observed (data not shown). In keeping with this, the tight junction-associated protein ZO-1 was not demonstrable by immunohistochemistry (Fig. 3b). The tracer ruthenium red was found to be able to penetrate in the lateral intercellular space from the apical compartment beyond the subapical region, indicating the lack of a fully developed tight junctional barrier (Fig. 3e).

Adherens junctions. Conventional immunofluorescence microscopy revealed that E-cadherin, α-catenin, β-catenin and plakoglobin are expressed by HEC monolayers (data not shown). Confocal microscopy showed that E-cadherin (Fig. 4a), α-catenin (Fig. 4c), β-catenin (Fig. 4e), and plakoglobin (Fig. 4g) were confined to cell-to-cell contacts.

Fig. 4. Confocal vertical images of HEC-1-A monolayers (**a, c, e, g**) and RL95-2 monolayers (**b, d, f, h**) after staining with monoclonal antibody to E-cadherin (**a, b**), α-catenin (**c, d**), β-catenin (**e, f**), and plakoglobin (**g, h**). Vertical sections reveal that E-cadherin, α-catenin, β-catenin, and plakoglobin were confined to cell-to-cell contacts in HEC-1-A cells. In RL95-2 cells, only β-catenin was confined to the lateral plasma membrane, while E-cadherin, α-catenin, and plakoglobin were located at all plasma membrane domains. Note that α-catenin fluorescence (**d**) as well as plakoglobin fluorescence (**h**) suggest an intracellular localization, too. *Arrows* mark the position of cell-to-cell contacts in monolayers. – oo Coverslip. – *Stars:* Growth medium. – Bar 10 μm.

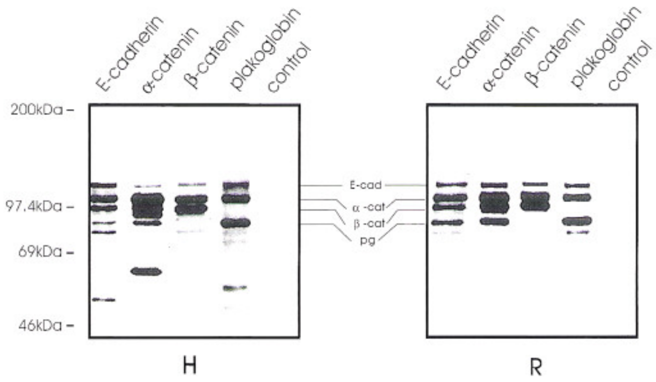

Fig. 5. Immunoprecipitations of E-cadherin/catenin complexes from radiolabeled HEC-1-A cells (H) and RL95-2 cells (R). Cell extracts were immunoprecipitated with anti-E-cadherin (E-cadherin), anti-α-catenin (α-catenin), anti-β-catenin (β-catenin), and anti-plakoglobin (plakoglobin). In both HEC-1-A cells and RL95-2 cells two different E-cadherin/catenin complexes were detected, i.e. E-cadherin (E-cad) and α-catenin (α-cat) in association with β-catenin (β-cat) as well as E-cadherin and α-catenin in association with plakoglobin (pg). Note additional proteins in HEC-1-A cell extracts when immunoprecipitated with anti-E-cadherin, anti-α-catenin, and anti-plakoglobin. The proteins were resolved by SDS-PAGE using 7.5% acrylamide gels. Reference proteins used for coelectrophoresis are ^{14}C-methylated myosin (200000 Da), ^{14}C-methylated phosphorylase B (97400 Da), ^{14}C-methylated bovine serum albumin (69000 Da), and ^{14}C-methylated ovalbumin (46000 Da).

When cell lysates from metabolically labeled HEC cells were subjected to immunoprecipitation using antibodies specific for E-cadherin, four major protein bands of molecular weight 120000 Da, 102000 Da, 88000 Da, and 80000 Da were detected (Fig. 5). When such anti-E-cadherin immunoprecipitate gels were blotted and subsequently stained with anti-E-cadherin, anti-α-catenin, anti-β-catenin, and anti-plakoglobin, it was possible to identify the major bands as E-cadherin (120000 Da), α-catenin (102000 Da), β-catenin (88000 Da), and plakoglobin (80000 Da) (data not shown). Immunoprecipitates with antibody specific to α-catenin and subsequent immunostaining with anti-E-cadherin, anti-α-catenin, anti-β-catenin, and anti-plakoglobin revealed E-cadherin, α-catenin, β-catenin, and plakoglobin (Fig. 5). Immunoprecipitates collected with anti-β-catenin or anti-plakoglobin differed, however, insofar as either β-catenin or plakoglobin was not detectable in the alternative immunoprecipitate. This indicates that two different E-cadherin-catenin complexes are present in HEC cells, one composed of E-cadherin, α-catenin and β-catenin, the other of E-cadherin, α-catenin and plakoglobin. Beyond that, immunoprecipitations collected with anti-E-cadherin, anti-α-catenin, and plakoglobin revealed additional bands in the range of 60000 Da to 50000 Da which are, however, not identified so far.

RL cells showed, like HEC cells, the presence of E-cadherin, α-catenin, β-catenin and plakoglobin (data from conventional immunohistochemistry; not shown). Confocal microscopy revealed that E-cadherin (Fig. 4b), α-catenin (Fig. 4d), and plakoglobin (Fig. 4h) were colocalized in all plasma membrane domains of these cells (in contrast to HEC cells), while β-catenin (Fig. 4f) was localized in lateral membrane domains of adjacent cells. Moreover, plakoglobin fluorescence (Fig. 4h) and also α-catenin fluorescence (Fig. 4d) suggest an intracellular localization of plakoglobin and α-catenin, too.

When cell lysates from metabolically labeled RL cells were subjected to immunoprecipitations with antibodies against E-cadherin, α-catenin, β-catenin, and plakoglobin (Fig. 5) the same pattern of bands was obtained as with HEC cells. In contrast to HEC cells, however, RL cells lacked additional bands in the range of 60000 Da to 50000 Da. Comparison of cell lines leads to the conclusion that in both cell types two different E-cadherin-catenin complexes are present, one complex containing E-cadherin and α-catenin in association with β-catenin, the other E-cadherin and α-catenin in association with plakoglobin.

Actin distribution. Actin filament arrangements as seen after staining with TRITC-conjugated phalloidin differed in RL and HEC cells as shown in Figure 6.

HEC cells showed spot-like actin staining associated with the microvilli of the apical plasma membrane (Fig. 6a), peripheral bands which surrounded the margin of the cells (Figs. 6a, b, d) as well as stress fibers which ran longitudinally at the base of the cells (Fig. 6b).

A different actin organization was observed in RL cells (Figs. 6c, e). In contrast to HEC cells, microvilli-associated staining as well as stress fibers could not be observed in RL cells (Fig. 6c). Nevertheless, cells showed actin staining along the entire cell surface and diffuse staining within the cytoplasm. The appearance of actin staining beneath the plasma

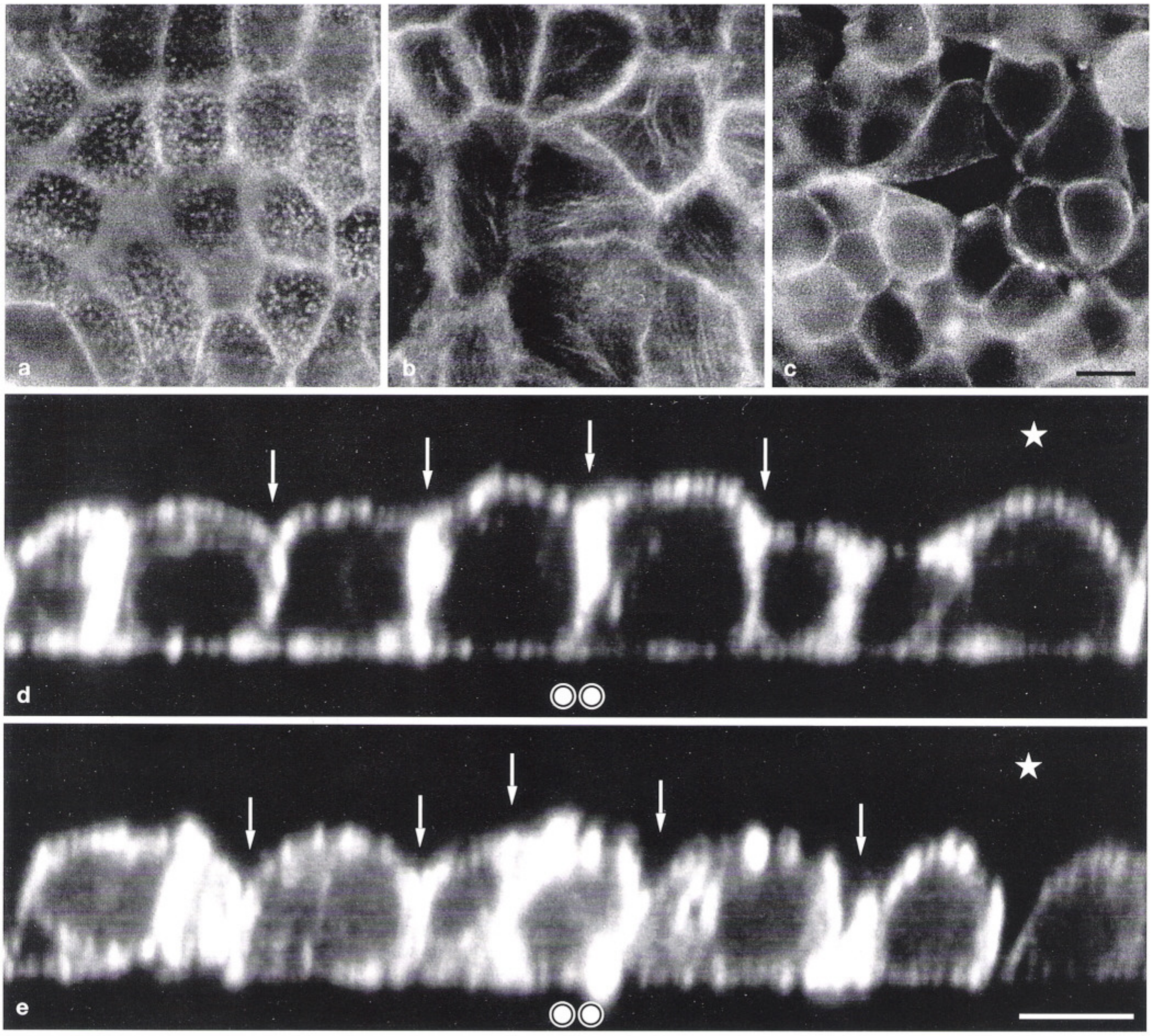

Fig. 6. Actin staining of HEC-1-A monolayers (**a, b,** conventional microscopy; **a:** focused apically; **b:** focused basally; **d:** confocal vertical image) and RL95-2 monolayers (**c,** conventional microscopy; **e,** confocal vertical image) with TRITC-conjugated phalloidin. Note that HEC-1-A cells but not RL95-2 cells show fluorescence associated with microvilli (**a**), peripheral bands, and stress fibers (**b**). *Arrows* mark the position of cell-to-cell contacts in vertical images. – oo Coverslip. – *Stars:* Growth medium. – Bars 10 μm (**a–c**), 10 μm (**d, e**).

membrane varied in different regions of the same cell, i.e. in some areas large clumps of fluorescent material were seen, in other areas only small spots (Fig. 6e).

Desmosomes. In HEC cells, transmission electron microscopy showed typical desmosomes localized basally to the tight junctions (Fig. 1c). By immunohistochemistry, desmoplakin I could be identified in punctate arrays (Fig. 7a), restricted along cell-to-cell contacts, i.e. at the lateral plasma membrane (Fig. 7c).

In RL cells, lateral plasma membranes usually lacked typical desmosomes (Fig. 1d) which were only occasionally found. Desmoplakin I was demonstrable immunhistochemically (Fig. 7b) and, in contrast to HEC cells, was not restricted to cell-to-cell contacts but also seen in the luminal and basal membranes (data not shown). Further electron microscopy studies (e.g. [9]) will help understand the distribution and formation of desmosomes in these cells.

Discussion

RL95-2 cells represent a human uterine epithelial cell line which displays adhesive properties of its apical plasma membrane for trophoblast-type cells [27]. In this respect, RL cells might act as an in vitro model for the receptive uterine epithelium. Recent studies have indicated that apical adhesiveness of RL cells is associated with a low degree of their apical-basal cell polarity [50, 51]. Focusing on steps leading to modulation of cell polarity in vivo, we mapped cell-to-cell contacts in RL cells and found defects of integrity of their junctional complex. RL cells showed a lack of ZO-1 expression and tracer leakiness of the paracellular pathway, and atypical features in adherens junctions. Additionally, the actin-based cytoskeleton lacked a polar organization. Moreover, RL cells expressed desmoplakin but lacked mostly well-formed desmosomes.

Although expressing E-cadherin, α-catenin, β-catenin, and plakoglobin, RL cells lack well-organized adherens junctions. On the other hand, evidence was seen for an atypical distribution of these molecules, i.e. random localization of E-cadherin, α-catenin and plakoglobin at all plasma membrane domains but restriction of localization of β-catenin to the lateral domains. E-cadherin is recognized as a master molecule for the maintenance of epithelial integrity and polarized organization [17, 36]. The cytoplasmic domain of E-cadherin interacts with a family of submembranous plaque proteins of which are presently known α-catenin, β-catenin, plakoglobin [40] and p120cas described recently [44]. These plaque proteins interact in a yet unidentified way with structural components of the actin cytoskeleton [40, 48]. The random localization of E-cadherin, α-catenin and plakoglobin on the one side and the

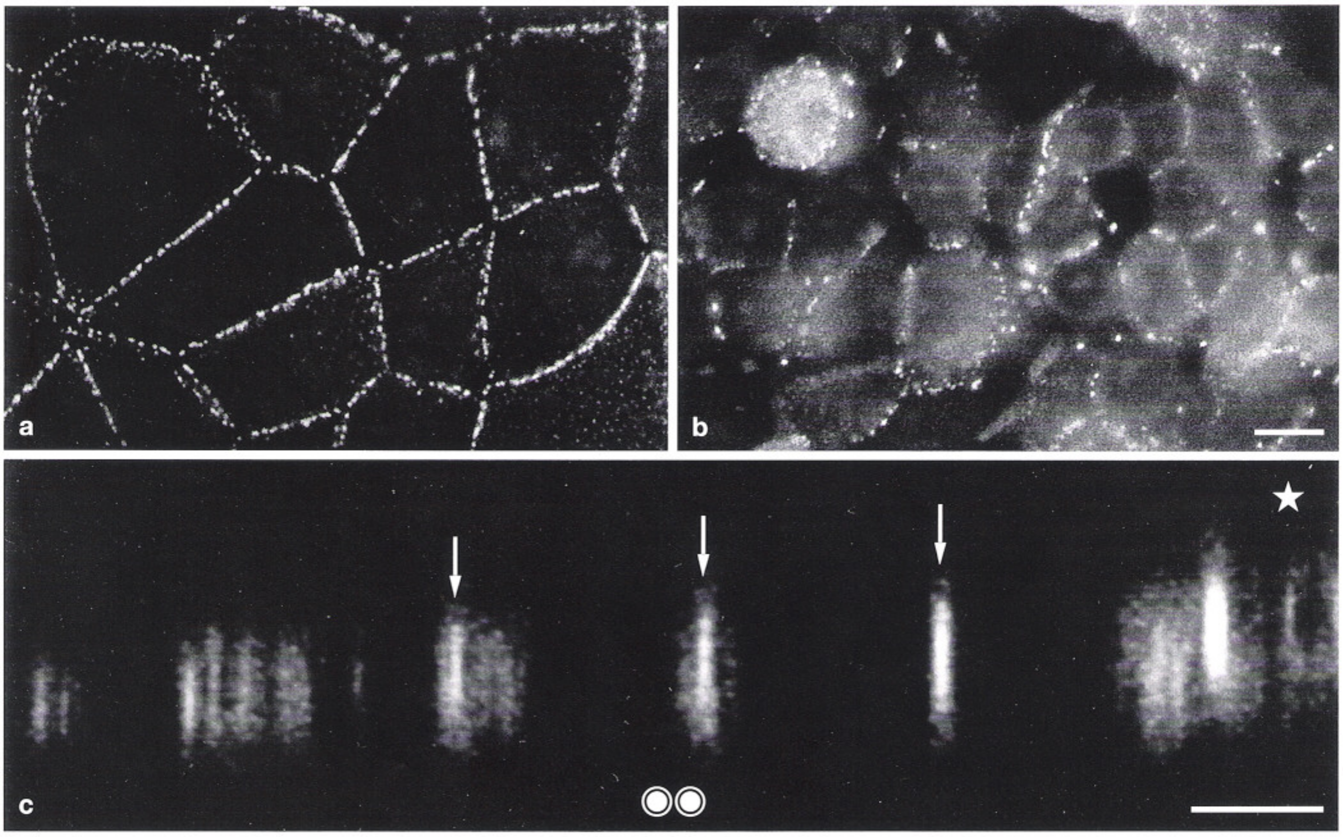

Fig. 7. Immunostaining of HEC-1-A monolayers (**a**, conventional microscopy; **c**, confocal vertical image) and RL95-2 monolayers (**b**, conventional microscopy) with antibodies to desmoplakin I. Desmoplakin was found in punctate arrays along the cell-to-cell contacts in HEC-1-A cells. In RL95-2 cells staining was not only restricted to lateral membrane domains of adjacent cells but also seen in the apical and basal membrane domains. *Arrows* mark the position of cell-to-cell contact in vertical images. – oo Coverslip. – *Star:* Growth medium. – Bars 10 μm (**a**, **b**), 10 μm (**c**).

lateral localization of β-catenin on the other side might be due to (partial) disassembly of the complexes formed between E-cadherin, plaque proteins and the actin filament network [3, 22, 24, 25, 39, 45]. The intracellular localization of plakoglobin and α-catenin (beyond their localization in plasma membranes) might point to internalization of distinct plaque components in RL cells. A decrease of function of adherens junctions is supposed to be controlled by the level of protein tyrosine phosphorylation. For example, transformation of MDCK cells (an epithelial cell line) with v-src or inhibition of protein tyrosine phosphatase activity with pervanadate induced elevation of tyrosine phosphorylation of catenins and functional inactivation of cadherin-mediated cell-to-cell adhesion accompanied by dissociation of the junctional actin bundle from the membrane and followed by rounding up of the apical cell surfaces and perturbation of epithelial monolayer morphology [2, 18, 34, 44, 53, 54]. Interestingly, complexes formed between E-cadherin, α-catenin and β-catenin, and E-cadherin, α-catenin and plakoglobin are detectable in RL cells. Thus, combined evidence from confocal immunofluorescence microscopy and from immunoprecipitations suggests that E-cadherin/plakoglobin complexes are located randomly and E-cadherin/β-catenin complexes are located laterally in these cells. The differential distribution of both complexes in the same cell might point to differences in their association with the actin-based cytoskeleton [32, 52]. Processes leading to tyrosine phosphorylation of different catenins and thus inactivating the association of distinct catenins with actin filaments might be involved here [18, 23]. This leads to the question whether E-cadherin, α-catenin and β-catenin or E-cadherin, α-catenin and plakoglobin might affect the epithelial phenotype by directly or indirectly influencing the generation of structurally and functionally distinct membrane domains. Indeed, cells can differentially regulate the organization of cadherin and associated cytoplasmic molecules at junctions in relation to different functional requirements. In vascular endothelial cells assembly and disassembly of intercellular junctions have been described to comprise several steps that are regulated differently. Loose junctions as in early confluent cells are characterized by cadherin, α-catenin, and β-catenin deposition at contact sites, and plakoglobin is not found here. Stable junctions as in tightly confluent cells are characterized by plakoglobin localization at intercellular contact sites. These data suggest that while cadherin, α-catenin, and β-catenin complexes can function as early recognition mechanisms between endothelial cells, the strength of the cell-to-cell contact can be modulated by plakoglobin accumulation at junctions [29]. Moreover, regulated expression of different cadherin family members might lead to specialized cell phenotypes as shown in the retinal pigment epithelium system [33].

RL cells did not only show a modulation of adherens junctions but also alterations of tight junctions as they are characterized by a lack of ZO-1 expression and tracer leakiness of the paracellular pathway. It can be assumed that the level of protein tyrosine phosphorylation influences adherens junctions as well as tight junctions. Although pervanadate had no effect on ZO-1 immunostaining in MDCK cells [54] and expression of low levels of the tyrosine kinase v-src had no apparent effect on the thin section electron microscopic appearance of tight junctions [55], phosphorylation of tight junction associated proteins caused an increase in the ionic permeability in these cells [2, 47]. The apolar cytoskeletal architecture we observed in RL cells might point to an involvement of the actin cytoskeleton in tight junction modulation. Indeed, disruption of tight junctions (and of adherens junctions), possibly leading to a loss of apical-basal cell polarity, might be generated by disassembly of the actin-based cytoskeleton as shown by antimycin-A-generated ATP depletion in kidney epithelium-derived cell lines. Following a redistribution of the actin microfilament network and a disruption of the cortical cytoskeleton, the surface membrane undergoes extensive alterations in microvillous morphology, disruption of cellular junctions and loss of membrane polarity. With regard to the opening of tight junctions, lateral migration of domain-specific components could occur, resulting in loss of surface membrane polarity, i.e. membrane lipids and proteins are able to redistribute across domains. Na^+/K^+-ATPase, untethered from the cortical cytoskeleton, redistributes into the apical domain, while the apical marker protein leucine aminopeptidase redistributes into the basolateral domain [30, 42]. Similarly, investigations using the renal epithelial cell line BS-C-1 oxidatively stressed by H_2O_2 treatment have revealed that disruption of focal adhesions with loss of talin from the basal cell surface untethers the associated integrins, allowing them to redistribute into the apical domain [15]. In vivo, moderate restructuring of the actin-based cytoskeletal network occurs in response to a variety of extracellular and intracellular signals. One of them might be growth factors like epidermal growth factor which cooperate with c-src tyrosine kinase and GTPase-activating proteins [6].

An interesting question is whether the interdependent phenomena of a remodelling of cell-to-cell adhesion system and the rearrangements of the actin cytoskeleton might depend on a master gene program which, triggered by steroids, controls the development of the receptive state in the uterine epithelium [10–12]. Such master genes could be related to those postulated to govern epithelium-to-mesenchyme transformation in embryology and cancer progression [19, 43, 46]. Apart from E-cadherin mentioned earlier, the gene encoding fibroblast-specific protein 1 (FSP1) [49] has been proposed to represent such a master gene [20]. Signals such as tumor-promoting phorbol esters, oncoproteins, and growth factors may in turn control master gene activation in these systems. It will be a challenge for further investigations on human uterine epithelial cells to look for direct evidence whether the gene program for the epithelial phenotype is indeed undergoing a modulation in connection with the acquisition of receptivity for trophoblast.

Acknowledgements. The skillfull technical assistance of Birgit Nowak, Dorothea Schünke, and Ulrike Tlolka is gratefully acknowledged. We also wish to thank Dr. J. Behrens and Dr. J. Kartenbeck for the generous gifts of antibodies. We would like to thank Dr. G. Bruder and Dr. J. Kartenbeck for help with the choice of cytokeratin antibodies and to Dr. R. Moll for helpful comments to intermediate filament analysis. We are also obliged to Prof. Dr. C. Streffer (Director of the Institute for Radiation Biology of the University, Essen/Germany) for making available to us the confocal microscopy unit and for his interest in this work.

References

[1] Albers, A., M. Thie, H.-P. Hohn, H.-W. Denker: Differential expression and localization of integrins and CD44 in the membrane domains of human uterine epithelial cell during the menstrual cycle. Acta Anat. **153,** 12–19 (1995).

[2] Behrens, J., L. Vakaet, R. Friis, E. Winterhager, F. van Roy, M. M. Mareel, W. Birchmeier: Loss of epithelial differentiation and gain of invasiveness correlates with tyrosine phosphorylation of the E-cadherin/β-catenin complex in cells transformed with a temperature-sensitive-v-SRC gene. J. Cell Biol. **120,** 757–766 (1993).

[3] Butz, S., R. Kemler: Distinct cadherin-catenin complexes in Ca^{2+}-dependent cell-cell adhesion. FEBS Lett. **355,** 195–200 (1994).

[4] Butz, S., S. Rawer, W. Rapp, U. Birsner: Immunization and affinity purification of antibodies using resin-immobilized lysine-branched synthetic peptides. Pept. Res. **7,** 20–23 (1994).

[5] Butz, S. J. Stappert, H. Weissig, R. Kemler: Plakoglobin and β-catenin: distinct but closely related. Science **257,** 1142–1144 (1992).

[6] Chang, J.-H., S. Gill, J. Settleman, S. J. Parsons: c-Src regulates the simultaneous rearrangement of actin cytoskeleton, p190RhoGAP, and p120Ras GAP following epidermal growth factor stimulation. J. Cell Biol. **130,** 355–368 (1995).

[7] Cowin, P., H.-P. Kapprell, W. W. Franke: The complement of desmosomal plaque proteins in different cell types. J. Cell Biol. **101,** 1442–1454 (1985).

[8] Cross, R. H. M.: A reliable epoxy resin mixture and its application in routine biological transmission electron microscopy. Micron Microsc. Acta **20,** 1–7 (1989).

[9] Demlehner, M. P., S. Schäfer, C. Grund, W. W. Franke: Continual assembly of half-desmosomal structures in the absence of cell contacts and their frustrated endocytosis: a coordinated sisyphus cycle. J. Cell Biol. **131,** 745–760 (1995).

[10] Denker, H.-W.: Trophoblast-endometrial interactions at embryo implantation: a cell biological paradox. In: H.-W. Denker, J. D. Aplin (eds.): Trophoblast Invasion and Endometrial Receptivity. Novel Aspects of the Cell Biology of Embryo Implantation. Trophoblast Research Vol. 4. pp. 3–29. Plenum Medical Book Comp. New York, London 1990.

[11] Denker, H.-W.: Implantation: a cell biological paradox. J. Exp. Zool. **266,** 541–558 (1993).

[12] Denker, H.-W.: Cell biology of endometrial receptivity and of trophoblast-endometrial interactions. In: S. R. Glasser, J. Mulholland, A. Psychoyos (eds.): Endocrinology of Embryo-Endometrium Interactions. pp. 17–32. Plenum Press. New York, London 1994.

[13] Eckert, W., J. Kartenbeck: Methoden der Zell- und Molekularbiologie. Teil I. Springer-Verlag. New York, London 1996.

[14] Frixen, U. H., J. Behrens, M. Sachs, G. Eberle, B. Voss, A. Warda, D. Löchner, W. Birchmeier: E-cadherin-mediated cell-cell adhesion prevents invasiveness of human carcinoma cells J. Cell Biol. **113,** 173–185 (1991).

[15] Gailit, J., D. Coflesh, I. Rabiner, J. Simone, M. S. Goligorsky: Redistribution and dysfunction of integrins in cultured renal epithelial cells exposed to oxidative stress. Am. J. Physiol. **264,** F149–F157 (1993).

[16] Glasser, S., J. Mulholland: Receptivity is a polarity dependent special function of hormonally regulated uterine epithelial cells. Microsc. Res. Techn. **25,** 106–120 (1993).

[17] Gumbiner, B., B. Stevenson, A. Grimaldi: The role of the cell adhesion molecule uvomorulin in the formation and maintenance of the epithelial junctional complex. J. Cell Biol. **107,** 1575–1587 (1988).

[18] Hamaguchi, M., N. Matsuyoshi, Y. Ohnishi, B. Gotoh, M. Takeichi, Y. Nagai: p60v-src causes tyrosine phosphorylation and inactivation of the N-cadherin-catenin cell adhesion system. EMBO J. **12,** 307–314 (1993).

[19] Hay, E. D.: Epithelial-mesenchymal transitions. Semin. Dev. Biol. **1,** 347–356 (1990).

[20] Hay, E. D.: An overview of epithelio-mesenchymal transformation. Acta Anat. **154** (1) (in press, 1996).

[21] Herrenknecht, K., M. Ozawa, C. Eckerskom, F. Lottspeich, M. Lenter, R. Kemler: The uvomorulin-anchorage protein α catenin is a vinculin homolgue. Proc. Natl. Acad. Sci. USA **88,** 9156–9160 (1991).

[22] Hinck, L., I. S. Näthke, J. Papkoff, W. J. Nelson: Dynamics of cadherin/catenin complex formation: novel protein interactions and pathways of complex assembly. J. Cell Biol. **125,** 1327–1340 (1994).

[23] Hoschützky, H., H. Aberle, R. Kemler: β-Catenin mediates the interaction of the cadherin-catenin complex with epidermal growth factor receptor. J. Cell Biol. **127,** 1375–1380 (1994).

[24] Hülsken, J., J. Behrens, W. Birchmeier: Tumor-suppressor gene products in cell contacts: the cadherin-APC-armadillo connection. Curr. Opin. Cell Biol. **6,** 711–716 (1994).

[25] Hülsken, J., W. Birchmeier, J. Behrens: E-cadherin and APC compete for the interaction with beta-catenin and the cytoskeleton. J. Cell Biol. **127,** 2061–2069 (1994).

[26] Jansen, R. P. S., M. Turner, E. Johannisson, B. M. Landgren, E. Dicfalusy: Cyclic changes in human endometrial surface glycoproteins: a quantitative histochemical study. Fertil. Steril. **44,** 85–91 (1985).

[27] John, N. J., M. Linke, H.-W. Denker: Quantitation of human choriocarcinoma spheroid attachment to uterine epithelial cell monolayers. In Vitro Cell. Dev. Biol. **29**A, 461–468 (1993).

[28] Laemmli, U. K.: Cleavage of structural proteins during the assembly of the head of bacteriophage T4. Nature **227,** 680–685 (1970).

[29] Lampugnani, M. G., M. Corada, L. Caveda, F. Breviario, O. Ayalon, B. Geiger, E. Dejana: The molecular organization of endothelial cell to cell junctions: differential association of plakoglobin, β-catenin, and α-catenin with vascular endothelial cadherin (VE-cadherin). J. Cell Biol. **129,** 203–217 (1995).

[30] Leiser, J., B. A. Molitoris: Disease processes in epithelia: the role of the actin cytoskeleton and altered surface membrane polarity. Biochim. Biophys. Acta **1225,** 1–13 (1993).

[31] Luft, J. H.: Ruthenium red and violet. I. Chemistry, purification, methods of use for electron microscopy and mechanism of action. Anat. Rec. **171,** 347–368 (1971).

[32] Luna, E. J., A. L. Hitt: Cytoskeleton-plasma membrane interactions. Science **258,** 955–964 (1992).

[33] Marrs, J. A., C. Andersson-Fisone, M. C. Jeong, L. Cohen-Gould, C. Zurzolo, I. R. Nabi, E. Rodriguez-Boulan, W. J. Nelson: Plasticity in epithelial cell phenotype: modulation by expression of different cadherin cell adhesion molecules. J. Cell Biol. **129,** 507–519 (1995).

[34] Matsuyoshi, N., S. Hamaguchi, S. Taniguchi, A. Nagafuchi, S. Tsukita, M. Takeichi: Cadherin-mediated cell-cell adhesion is pertubed by v-src tyrosine phosphorylation in metastatic fibroblasts. J. Cell Biol. **118,** 703–714 (1992).

[35] Matthews, C. J., C. P. F. Redfern, B. H. Hirst, E. J. Thomas: Characterization of human purified epithelial and stromal cell from endometrium and endometriosis in tissue culture. Fertil. Steril. **57,** 990–997 (1992).

[36] McNeill, H., M. Ozawa, R. Kemler, W. J. Nelson: Novel function of the cell adhesion molecule uvomorulin as an inducer of cell surface polarity. Cell **62,** 309–316 (1990).

[37] Moll, R., R. Levy, B. Czernobilsky, P. Hohlweg-Majert, G. Dahlenbach-Hellweg, W. W. Franke: Cytokeratins of normal epithelia and some neoplasms of the female genital tract. Lab. Invest. **49,** 599–610 (1983).

[38] Murphy, C. R.: The plasma membrane of uterine epithelial cells: structure and histochemistry. Progr. Histochem. Cytochem. **27,** 1–66 (1993).

[39] Näthke, I. S., L. Hinck, J. R. Swedlow, J. Papkoff, W. J. Nelson: Defining interactions and distributions of cadherin and catenin complexes in polarized epithelial cells. J. Cell Biol. **125,** 1341–1352 (1994).

[40] Nagafuchi, A., S. Tsukita, M. Takeichi: Transmembrane control of cadherinmediated cell-cell adhesion. Semin. Cell Biol. **4,** 175–181 (1993).

[41] Ozawa, M., H. Baribault, R. Kemler: The cytoplasmic domain of the cell adhesion molecule uvomorulin associates with three independent proteins structurally related in different species. EMBO J. **8,** 1711–1717 (1989).

[42] Paller, M. S.: Lateral mobility of Na, K-ATPase and membrane lipids in renal cells. Importance of cytoskeletal integrity. J. Membr. Biol. **142,** 127–135 (1994).

[43] Reichmann, E.: Oncogenes and epithelial cell transformation. Semin. Cancer Biol. **5,** 157–165 (1994).

[44] Reynolds, A. B., J. Daniel, P. McCrea, M. J. Wheelock, J. Wu, Z. Zhang: Identification of a new catenin: the tyrosine kinase substrate p120cas associates with E-cadherin complexes. Mol. Cell. Biol. **14,** 8333–8342 (1994).

[45] Rubinfeld, B., B. Souza, I. Albert, S. Munemitsu, P. Polakis: The APC protein and E-cadherin form similar but independent complexes with alpha-catenin, beta-catenin, and plakoglobin. J. Biol. Chem. **270,** 5549–5555 (1995).

[46] Savagner, P., B. Boyer, A. M. Valles, J. Jouanneau, J. P. Thiery: Modulations of the epithelial phenotype during embryogenesis and cancer progression. Cancer Treat. Res. **71,** 229–249 (1994).

[47] Staddon, J. M., K. Herrenknecht, C. Smales, L. L. Rubin: Evidence that tyrosine phosphorylation may increase tight junction permeability. J. Cell Sci. **108,** 609–619 (1995).

[48] Stappert, J., R. Kemler: Intracellular association of adhesion molecules. Curr. Opin. Neurobiol. **3,** 60–66 (1993).

[49] Strutz, F., H. Okada, C. W. Lo, T. Danoff, R. L. Carone, J. E. Tomaszewski, E. G. Neilson: Identification and characterization of a fibroblast marker: FSP1. J. Cell Biol. **130,** 393–405 (1995).

[50] Thie, M., A. Albers, H.-W. Denker: Endometrial receptivity: cell biological aspects. In: T. Mori, T. Aono, T. Tominaga, H. Hiroi (eds.): Perspectives on Assisted Reproduction. Serono Symposia Series Frontiers in Endocrinology Vol. 4. pp. 331–337. Ares-Serono Symposia. Christengraf S. r. I. Rome 1994.

[51] Thie, M., B. Harrach-Ruprecht, H. Sauer, P. Fuchs, A. Albers, H.-W. Denker: Cell adhesion to the apical pole of epithelium: a function of cell polarity. Eur. J. Cell Biol. **66,** 180–191 (1995).

[52] Tsukita, S., M. Itoh, A. Nagafuchi, S. Tonemura, S. Tsukita: Submembranous junctional plaque proteins include potential tumor suppressor molecules. J. Cell Biol. **123,** 1049–1053 (1993).

[53] Volberg, T., B. Geiger, Y. R. Dror, Y. Zick: Modulation of intercellular adherenstype junctions and tyrosine phosphorylation of their components in RSV transformed cultured chick lens cells. Cell Regul. **2,** 105–120 (1991).

[54] Volberg, T., Y. Zick, R. Dror, I. Sabanay, C. Gilon, A. Levitzki, B. Geiger: The effect of tyrosine-specific protein phosphorylation on the assembly of adherens-type junctions. EMBO J. **11,** 1733–1742 (1992).

[55] Warren, S. L., W. J. Nelson: Nonmitogenic morphoregulatory action of pp60v-src on multicellular epithelial structures. Mol. Cell. Biol. **7,** 1326–1337 (1987).